A Review of Integrated Motor Drive and Wide-Bandgap Power Electronics for High-Performance Electro-Hydrostatic Actuators

Woongkul Lee, *Student Member, IEEE*, Silong Li, *Member, IEEE*, Di Han, *Student Member, IEEE*, Bulent Sarlioglu, *Senior Member, IEEE*, Tatiana A. Minav, *Member, IEEE*, and Matti Pietola

***Abstract*— An integration of an electric motor and a drive with wide-bandgap (WBG) devices possesses numerous attractive features for electrified and decentralized actuation systems. The WBG devices can operate at a high-junction temperature (>170 °C) with improved efficiency due to fast switching speed and low on-state resistance. It also leads to better performance and higher power density electro-hydrostatic actuators (EHAs) than the traditional solutions, which are being widely adopted in industrial applications such as aerospace, robotics, automobiles, manufacturing, wind turbine, and off-road vehicles. This paper introduces and investigates the benefits of the integrated motor drive with the WBG-based power electronics for the EHA systems.**

***Index Terms*— Actuators, high-temperature operation, hydraulics, integrated motor drive (IMD), modularization, wide-bandgap (WBG) devices.**

I. Introduction

THE integrated motor drive (IMD) is a structural integration of an electric motor with a motor drive as a single unit, which improves power density with 10%–20% less volume and reduces 30%–40% of the overall system costs of installation and manufacturing [1]. The elimination of expensive components such as shielded connection cables, a separate housing for the inverter, a centralized controller cabinet, and high-voltage and current bus bars is the primary driving force in lowering the cost [2]. It also leads to an improved electromagnetic interference (EMI)/electromagnetic compatibility behavior due to the direct connection of the motor to the drive without additional cables [3].

The recent advancements in motor drive technology such as modularization and wide-bandgap (WBG) devices can significantly enhance the performance of the IMDs in fault tolerance, efficiency, power density, and high-temperature operation [2]–[5]. The WBG-based IMD is advantageous in many applications, and a huge potential lies in the electrification of actuators, which are being widely used in aerospace, robotics, automobiles, manufacturing, and off-road vehicles. The role of the electrified actuation system is becoming more critical especially in the automotive industry due to the rapidly growing interests in electric vehicles, off-road vehicles, and autonomous vehicles where the highly efficient and reliable steering, suspension, braking, and heavy-duty actuators are required [6]–[9].

The hydraulic actuator based on a cylinder is the most commonly used for linear transmission movement in industries where high-power density, robustness, reliability, high-temperature operation, lightweight, and low volume are required. However, the conventional combustion engine-driven hydraulic and electro-hydraulic (EH) actuators, as shown in Fig. 1(a), have fundamental limitations in achieving high efficiency due to the excessive throttled pressure loss and high heat generation in a servovalve [10].

Electromechanical (EM) actuator [11]–[13] and electro-hydrostatic actuator (EHA) [14], [15] were introduced to replace the conventional actuators. The EM actuator has the simplest structure, as illustrated in Fig. 1(b), and it provides the highest efficiency. However, the maximum power of the EM actuator is restricted. The high probability of jamming and wear of the mechanical transmission components also remain a concern [16].

The EHA utilizes an electric motor-driven bidirectional hydraulic pump in which the inefficient servovalve is eliminated, as shown in Fig. 1(c). The overall system efficiency of the EHA is higher than that of the EH due to the low parasitic losses while the hydraulic transmission system still provides high reliability with extremely high force capability. This new technology has been rapidly adopted in the aerospace industry since early 2000 [16]. However, the additional electric motor and power electronics of EHA increase the total volume and weight of the system, which degrades the total system power density, as shown in Fig. 2.

This paper investigates the use of WBG devices and IMD technology for reducing the volume and weight of EHA

Manuscript received February 19, 2018; revised April 22, 2018; accepted June 16, 2018. Date of publication July 10, 2018; date of current version September 19, 2018. This work was supported in part by the Wisconsin Electric Machines and Power Electronics Consortium (WEMPEC) and in part by the Academy of Finland funding (ArcticWEll and IZIF Projects). *(Corresponding author: Bulent Sarlioglu.)*

W. Lee and B. Sarlioglu are with the Department of Electrical and Computer Engineering, University of Wisconsin–Madison, Madison, WI 53706 USA (e-mail: woongkul.lee@gmail.com; sarlioglu@wisc.edu).

S. Li is with Ford Motor Company, Dearborn, MI 48120 USA.

D. Han is with Monolithic Power Systems, Inc., San Jose, CA 95119 USA.

T. A. Minav and M. Pietola are with the Department of Mechanical Engineering, Aalto University, FI-00076 Helsinki, Finland (e-mail: tatiana.minav@aalto.fi).

Digital Object Identifier 10.1109/TTE.2018.2853994

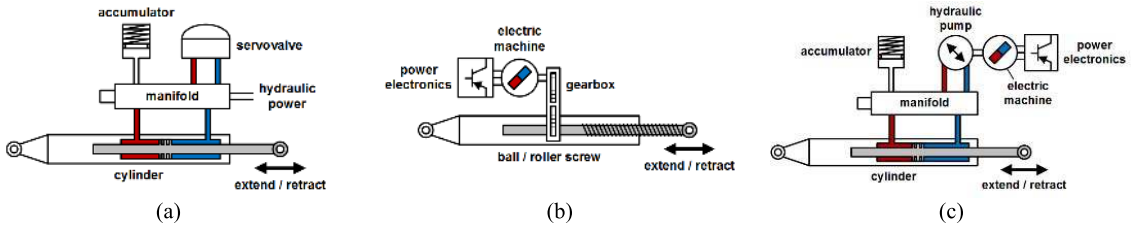

Fig. 1. Three different types of linear actuators. (a) Conventional hydraulic actuator (EH). (b) EM actuator. (c) EHA.

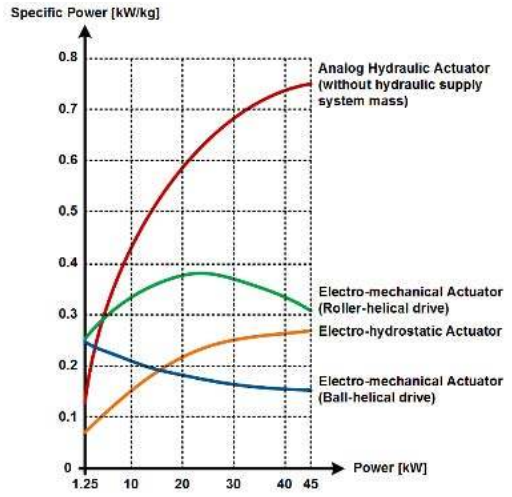

Fig. 2. Comparison of specific power versus output power of various actuator types for an actuator velocity of 300 mm/s replotted from [17].

and improving controllability in conjunction with high-temperature and fault-tolerant operation due to the compact integration and the modularized motor drive. Different motor designs for EHA with IMD are also introduced in detail.

II. Electro-Hydrostatic Actuators

The conventional hydraulic system consists of a hydraulic pump, an electric motor, and multiple cylinders connected by meter-in and meter-out valves. This structure is highly cost-effective due to the lowest number of the pump and the electric motor, but only applicable to a system with a strictly sequential working cycle [18]. The second level of individualization is the separate assignment of a variable displacement pump to each actuator while sharing a common prime mover. This structure reduces the overall number of valves since the motion control is carried out by variable displacement units, which can be switched to idling mode if needed [18].

The last level of individualization is the separate assignment of the EHA systems to each actuator. This configuration combines the best features of both hydraulic and electric technologies. It is also known as zonal or decentralized hydraulics—an approach first introduced in the aerospace industry. In a fully decentralized system, hydraulic pumps are disconnected from the engine and replaced with the hydraulic power packs distributed throughout the system [19].

There are three different structures of the EHA depending on the speed control capabilities of the electric motor and the hydraulic pump: 1) fixed pump displacement and variable motor speed; 2) variable pump displacement and fixed motor speed; and 3) variable pump displacement and variable motor speed [20]. The fixed pump displacement and variable motor speed configuration are most commonly used due to its structural simplicity and high efficiency. This actuation technology is the combination of the electric-to-mechanical power conversion and the mechanical-to-hydraulic power conversion, which ensures high reliability and high static force.

The WBG-IMD can play an essential role in the decentralized actuation system, where several motors and drives are required to manipulate the individual actuator. The overall volume and weight of the actuators can be significantly reduced while improving the performance and the overall system efficiency. The high-temperature operation capability and the improved EMI behavior would be the additional benefits from the use of WBG device and the compact integration.

III. Integrated Motor Drive With Wide-Bandgap Power Electronics

A. Configurations of Integrated Motor Drives

IMDs offer viable solutions for the increased demands of high-power density and highly efficient EHA systems. The principle concept of IMD is an integration of motor drive on or inside the motor housing, as shown in Fig. 3. There are four different IMD configurations, which have been reported in the literature: 1) radially housing-mounted (RHM); 2) axially housing-mounted (AHM); 3) radially stator iron-mounted (RSM); and 4) axially stator iron-mounted (ASM) [21], [22]. The radially mounted configurations are advantageous in high-speed motors, where the stack length tends to be longer than the stator diameter for low rotor inertia and low rotor tip speed [see Fig. 4(a)]. This configuration is also beneficial when the additional space needs to be allocated in an axial direction for a gearbox or a cooling fan.

On the other hand, the axially mounted configurations are preferable in high-torque motor, where the stator diameter tends to be longer than the stack length [see Fig. 4(b)]. The stator iron-mounted configurations provide more compact and seamless integration compared to the housing-mounted configurations, but they have several potential issues such as the limited space and additional cooling requirement due to high ambient temperature.

The example designs of four different configurations are shown in Figs. 5 and 6 with their specification summarized in Table I. There are a large number of commercialized RHM-IMDs and AHM-IMDs since these configurations

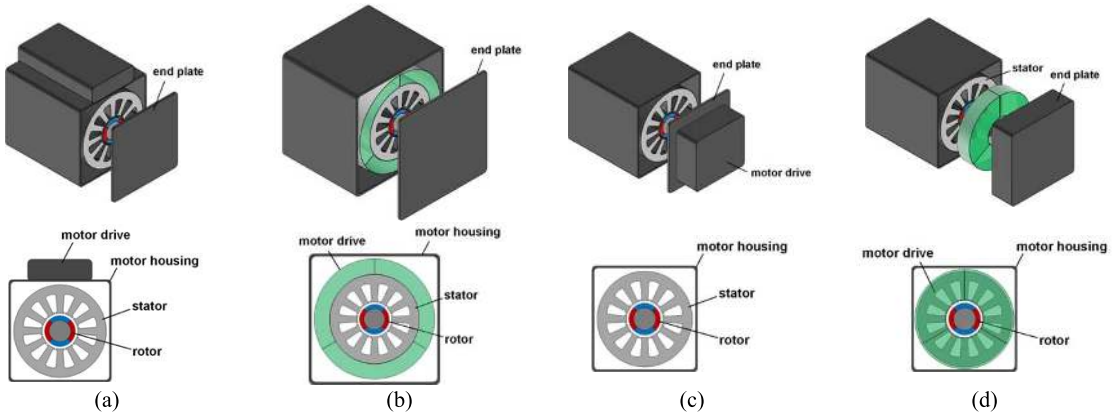

Fig. 3. Conceptual illustration of four different IMD configurations. (a) RHM. (b) RSM. (c) AHM. (d) ASM.

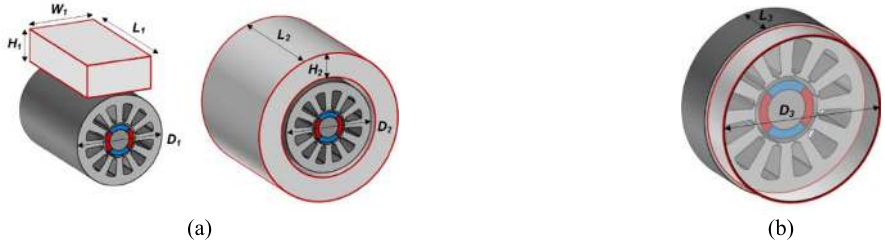

Fig. 4. Different integration methods of power electronics depending on the structure of the electric motors (space for power electronics highlighted in red). (a) Radially mounted for sausage-type motors ($L_1 > D_1$ and $L_2 > D_2$). (b) Axially mounted for pancake-type motors ($D_3 > L_3$).

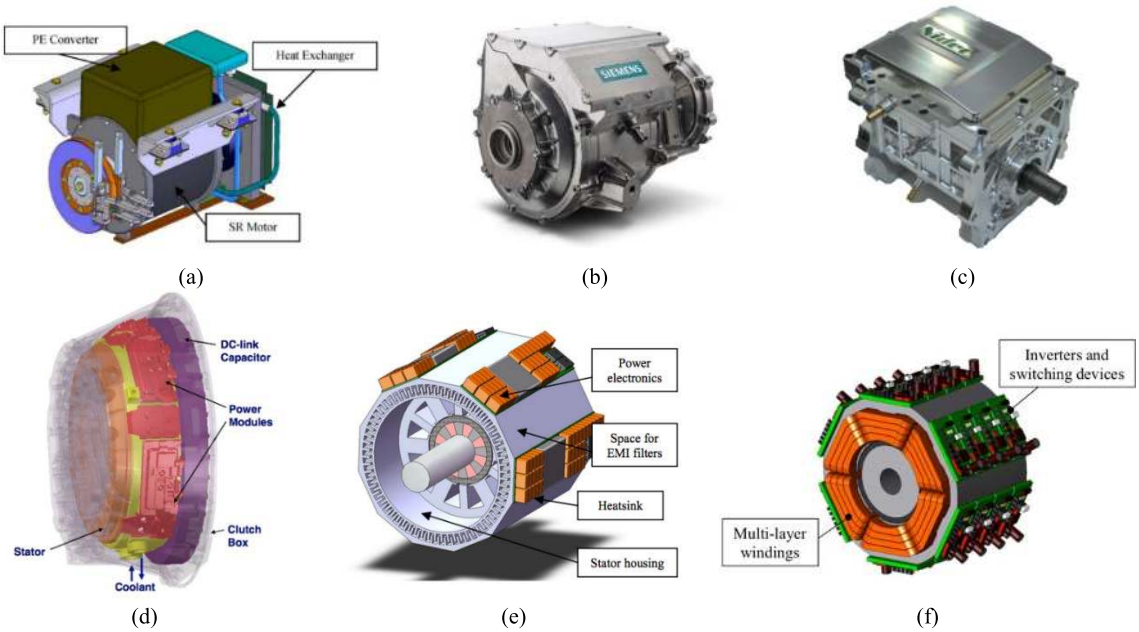

Fig. 5. Example designs of radially mounted IMDs. (a) RHM [23]. (b) RHM [24]. (c) RHM [25]. (d) RSM [3]. (e) RSM [26]. (f) RSM [27].

require the least modification on the existing motors and drives. Fig. 5(a) shows an RHM-IMD and Fig. 6(a) and (b) shows AHM-IMDs, where motors and drives are individually designed in separate housings and integrated. It is the simplest integration approach, which helps to avoid additional engineering challenges such as a thermal shielding between the motor and the drive and a modularization of motor drives for the integration on the curved motor surface.

More aggressive integration has been achieved by Siemens [Fig. 5(b)], Nidec [Fig. 5(c)], and Yaskawa [Fig. 6(c)], where the motor and the drive are more tightly integrated with cooling systems. Siemens claims that the overall system weight has been reduced by 10%–15% due to the elimination of the heavy connecting cables and the additional housing materials [24]. Nidec claims the volume and weight of the RHM-IMD that are 32% and 69% of the conventional motor

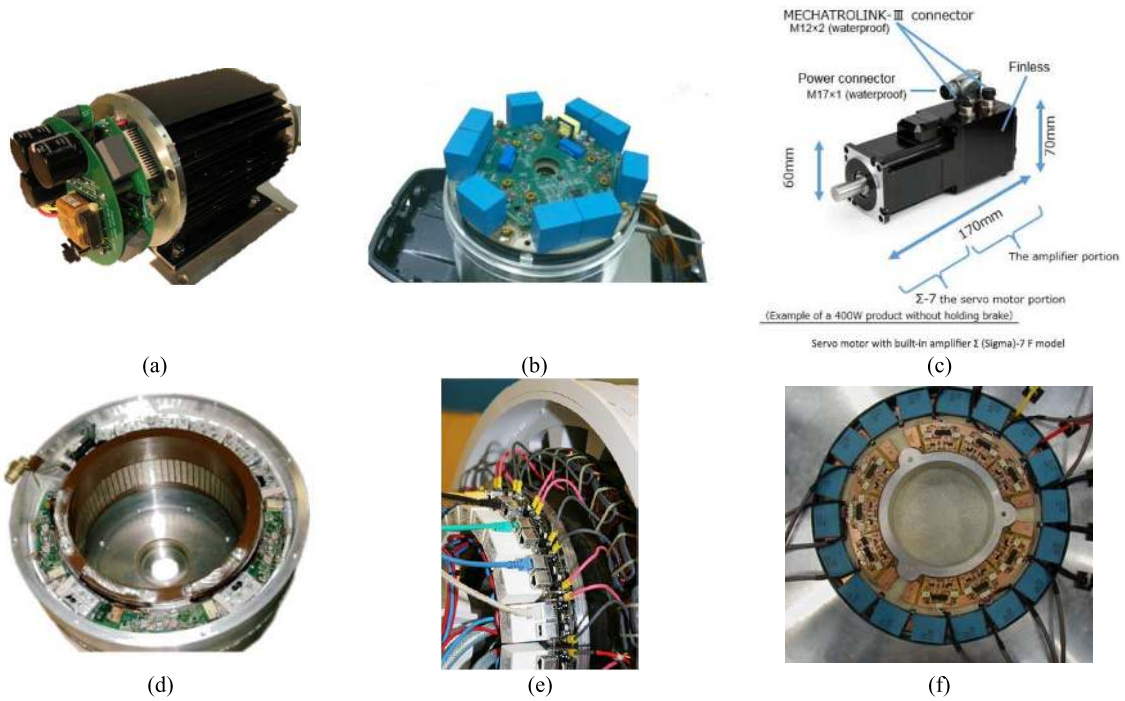

Fig. 6. Example designs of axially mounted IMDs. (a) AHM [28]. (b) AHM [29]. (c) AHM [30]. (d) ASM [3]. (e) ASM [31]. (f) ASM [34].

TABLE I
SUMMARY OF IMD SPECIFICATIONS

IMD type	Power rating [kW]	Motor type	Inverter type	Device type	Number of phase	Cooling	Reference / Fig. #
RHM	24	SRM	Asymmetrical half-bridge	Si	4	Liquid	[23] / Fig. 5(a)
	60	IM / SPM	2-level	Si	3	Liquid	[24] / Fig. 5(b)
	44	SRM	Asymmetrical half-bridge	SiC	3	Liquid	[25] / Fig. 5(c)
RSM	50	SPM	2-level modular	Si	3	Liquid	[3] / Fig. 5(d)
	50	SPM	Full-bridge	Si	6	Air	[26] / Fig. 5(e)
	0.02	SPM	2-level	Si	3	Air	[27] / Fig. 5(f)
AHM	2.7	SPM	2-level	Si	5	Air	[28] / Fig. 6(a)
	10.5	SPM	2-level	Si	3	Liquid	[29] / Fig. 6(b)
	55	IM	2-level segmented	Si	3	Liquid	[32]
	290	SPM	2-level modular	SiC	3	Liquid	[33]
	0.4	SPM	2-level	GaN	3	Air	[30] / Fig. 6(c)
ASM	90	IM	2-level modular	Si	3	Liquid	[3] / Fig. 6(d)
	1	IM	2-level modular	GaN	3	Air	[4]
	18	SPM	2-level modular	Si	6	Liquid	[5]
	67	SRM	Asymmetrical half-bridge	Si	5	Liquid	[31] / Fig. 6(e)
	30	IM	Matrix converter	Si	3	Air	[34] / Fig. 6(f)
	80	IPM	2-level modular	SiC	3	Liquid	[35]

Switched reluctance motor (SRM) / Induction motor (IM) / Surface permanent magnet motor (SPM) / Interior permanent magnet motor (IPM)

drive system, respectively [25]. The key enabling technologies for these IMDs are the advanced cooling system and the power switching devices. Siemens has invented a cooling system that creates a water screen between the motor and the drive for the thermal isolation. Nidec has developed a silicon carbide (SiC)-based motor drive, which can operate at high switching frequency and high junction temperature with significantly reduced volume and weight. Yaskawa has developed a compact and finless 3-kW gallium nitride (GaN)-based motor drive, which generates much fewer losses compared to the conventional drive [30].

Nidec has announced the next research plan toward a stator iron-mounted IMD, where the power electronics components are directly integrated on the motor stator iron. This configuration has more benefits than housing-mounted IMDs such as compactness, less housing material, and modularization, which is preferable for more seamless integration on the curved motor surface as conceptually illustrated in Figs. 5(d)–(f) and 6(d)–(f). However, it requires a highly sophisticated cooling system to prevent overheating of power electronics components. In [3], the modularized power electronics components have been placed on the top of the motor

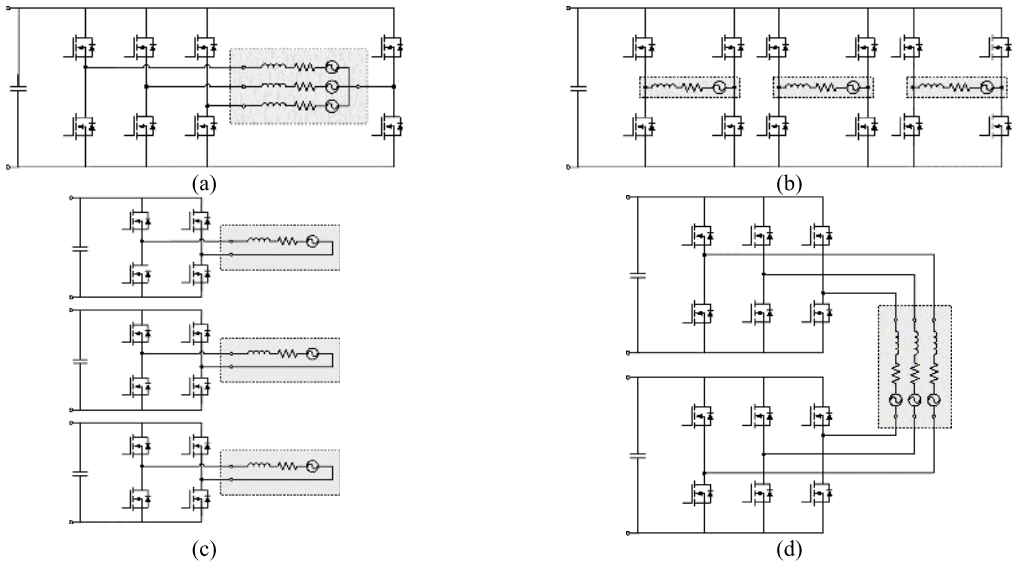

Fig. 7. Standard three-phase inverter and fault-tolerant three-phase inverter topologies for IMMDs. (a) Four-leg inverter. (b) Six-leg inverter with a single dc link. (c) Three single-phase inverters. (d) Cascaded inverter with separate dc links.

cooling jacket to create a thermal barrier between the motor and the drive, as shown in Fig. 5(d). In [26], a stator housing is integrated with a power electronics heat sink creating a single forced air cooling channel. In [34], the power electronics components are placed on the inside of the motor endplate, as shown in Fig. 6(f). The endplate is redesigned to have more fins to dissipate heat from the power electronics effectively.

B. Wide-Bandgap Devices for IMDs

WBG devices such as GaN and SiC provide several benefits for IMDs such as low switching and conduction losses, high-power density, and high-temperature operation. Both SiC and GaN devices have lower ON-state resistances as compared to Si MOSFETs at the ambient temperature of 25 °C. GaN devices, in general, have the lowest ON-state resistance, but as the ambient temperature increases up to 150 °C, SiC devices outperform any other types of devices, which make them ideal for the high-temperature operation. The price of the WBG device is still 2–3 times higher than that of the Si MOSFET, and GaN devices are generally more expensive than SiC devices due to the manufacturing complexity (reliability, current collapse, and packaging) and low market penetration. Nevertheless, the overall WBG-based IMD system cost can be significantly reduced from other parts such as cooling, connecting wires, passive components, control cabinet, and packaging, as shown in Figs. 5(c) and 6(c).

The performance of WBG devices in comparison with Si MOSFET and insulated-gate bipolar transistor (IGBT) has been extensively investigated over the last few years in many different applications [36]–[46]. In [36], 650-V GaN device was compared with Si CoolMOS where GaN showed 2–3 times faster switching speed with 2.5% higher efficiency at 300-kHz buck converter operation. When the 650-V SiC device was compared with Si-IGBT for automotive applications in [37], SiC power losses were 63% lower than that of Si-IGBT with 47% smaller footprint. In [3], the fundamental efficiency limits of Si, SiC, and GaN devices were analytically estimated and the WBG devices showed higher efficiency than that of Si devices in all frequency range from 10 kHz to 1 MHz. In [39], the efficiency of a SiC-based IMD was compared with a Si-based IMD for EHA applications, where the switching speed of SiC device was four times faster with 2% higher overall drive efficiency at 100 kHz as compared to the Si device. In [40], a 200-V GaN-based motor drive showed 4.89% higher efficiency than that of a Si-based motor drive, achieving 88.8% loss reduction from the switching devices.

In [42], a comprehensive analysis on a SiC-based and a Si-based 11-kW motor drives was conducted, where the SiC motor drive without any filter showed the lowest loss among other drives. However, the authors pointed out that the high *dv/dt* became an issue for a motor at some distance from the motor drive. In the IMD system, however, the *dv/dt* issue can be adequately mitigated due to the absence of the connection cables. In [43], it was reported that the efficiency of a GaN motor drive at light-load condition was significantly higher than that of Si-IGBT motor drive, which is critical in the pump applications. The light-load total system efficiency of GaN motor drive was 5%–20% higher than that of Si-IGBT motor drive. The same phenomenon was also observed in a SiC-based motor drive in [44]. At 15 kHz, SiC motor drive showed 20% higher efficiency as compared to that of Si-IGBT motor drive.

IV. Fault-Tolerant and High-Temperature Operation

A. Modularized and Fault-Tolerant Motor Drives

The modularization of the motor drive is one of the key features in IMDs. The modularized motor drives provide better installation on the curved surface of the stator lamination as well as the fault-tolerant operation, which is significant in the electrified actuator operation [47]–[50]. Fig. 7 shows

TABLE II
SiC SWITCHING DEVICE OPTIONS FOR IMD

Manufacturer	Cree	Infineon	Powerex (Mitsubishi)	STmicro	GeneSiC	Microsemi	USCi	ROHM	Semikron
Voltage [V]	900-1700	1200	1200	650-1200	600-1700	700-1200	650-1200	400-1700	1200-1700
Current [A]	5-300	10-300	20-100	12-100	10-160	25-80	10-40	4-120	25-550
T_{JMAX} [□C]	175	-	200	200	210	175	175	175	175
Structure†	M	M	M	M	JT	M	J / C	M	M
Packaging	TO-247/263	TO-247	Module	HiP247	Baredie / TO-46/257	TO-247	TO-247	TO-247	Module
Thermal Management	Heatsink	Heatsink	Heatsink	Heatsink	Heatsink	Heatsink	Heatsink	Heatsink	Heatsink
Availability	Yes	No	Yes	Yes	Yes	Yes	Yes	Yes	Yes
Comment	Leading provider	SBD	Modularized	High T_J	High T_J	-	Normally-on device	-	Augmented turn-off

M – normally-off (MOSFET) / J – normally-on (JFET) / C – normally-off (cascode) / JT – normally-off (junction transistor)

four different fault-tolerant inverter topologies [51], which are suitable for an integrated modular motor drive (IMMD) application. The additional TRIACs can be added to each topology to improve the fault-tolerant operation capability further [52]. The modularization of these inverter topologies can be achieved with multiple phase leg modules [Fig. 7(a)], multiple full-bridge inverter modules [Fig. 7(a) and (b)], or multiple three-phase inverter modules [Fig. 7(c)].

The four-leg inverter topology in Fig. 7(a) has an additional redundant inverter phase connected to the neutral point of an electric machine. This topology provides a single-phase open-circuit and a single-switch open-circuit fault tolerance for both induction and permanent magnet (PM) machines as reported in [53] and [54].

The six-leg inverter topology has three full-bridge inverters with a single dc-link capacitor, as shown in Fig. 7(b), which has a motor short-circuit fault [50] and a single-switch open-circuit fault tolerance [55]. For a single-switch short-circuit and a single-phase short-circuit fault tolerance, the additional TRIACs are required [50].

The three single-phase inverter topology [see Fig. 7(c)] has the same number of switches with the six-leg inverter, but it has three separate dc-link capacitors for each phase. It provides a dc-link capacitor fault tolerance as well as a single-phase open-circuit and a single-switch open-circuit fault tolerance.

The same number of switches can be reconfigured to form the cascaded inverter, as shown in Fig. 7(d). The connection of the inverter with the electric machine is essentially the same as the previous topologies except for the number of the dc-link capacitors. The benefit of having two separate dc-link capacitors is that there is no requirement for the zero-sequence current control [51]. This topology also provides a single-phase open-circuit and a single-switch open-circuit fault tolerance.

B. High-Temperature Operation

The EHAs are initially designed for an aerospace application. Therefore, the operating condition requirements are for harsh environments such as high altitude, high mechanical stress, and low temperatures in general. The most commercial actuation systems are designed to tolerate the temperature ranging from −18 °C to 71 °C.

With the current trend of individualization and integration, designers are facing higher requirements and challenges. When stationary or industrial applications are concerned, the typical operating condition is at the room temperature. The working temperature is defined by the oil, o-ring, and seal temperature. The safe temperature range for the oil is under 80 °C, which can slightly vary depending on the oil type and manufacturer.

Considering the mobile applications such as off-road machinery, the temperature variation range becomes much wider due to the environment temperature. Especially in a high-temperature working condition, the conventional hydraulic systems (open-circuit) utilize a high-volume tank for maintaining relatively constant oil temperature. In EHAs, which utilize a closed-circuit approach, the temperature control becomes a challenge due to the limited amount of oil. Therefore, the thermal balance between the components is important since the high temperature accelerates the degradation of the components.

For the motor drive, more aggressive cooling techniques can be used to dissipate the heat, but it will increase the overall volume and weight of the system. The WBG devices can be a better choice compared to Si devices since WBG devices inherently have higher operating temperature (>170 °C) than the conventional silicon (Si) devices. The commercially available WBG devices are summarized in Tables II and III, where SiC devices tend to have higher junction temperature than a typical junction temperature limit of Si devices (<150 °C) due to their low intrinsic charge carrier concentration [56]. The SiC devices also have three times higher thermal conductivity (lower thermal resistivity) than Si devices, which ensures the lower junction temperature rise for the same amount of power losses from the devices. Thus,

$$T_J - T_{\text{amb}} = P_{\text{loss}}(T_J)\theta_{J-A} \tag{1}$$

where T_J is the junction temperature, T_{amb} is the ambient temperature, $P_{\text{loss}}(T_J)$ is the power loss at T_J, and θ_{J-A} is the total junction-to-ambient thermal resistivity. In the case of GaN devices, the maximum junction temperature is typically the same as the conventional Si devices although there are few exceptions. It is important to note that the switching and conduction losses of the GaN devices are much lower than those of the Si devices, which helps to maintain the junction temperature low for the same operating condition.

TABLE III
GAN SWITCHING DEVICE OPTIONS FOR IMD

Manufacturer	EPC	Transphorm	GaN Systems	TI	Panasonic	VisIC	Avogy	POWDEC	Infineon / IR
Voltage [V]	15-300	600-1200	100 / 650	48 / 600	600	650	> 600	600 /1200	100-650
Current [A]	1-90	7-90	7.5-90	12	10-25	10-50	-	10	-
Substrate	Si	SiC	Si	Si	Si	Si	GaN	Sapphire	Si
T_{JMAX} [□C]	150	150	150	150	150	150	150	>200	-
Structure†	E	C	E	E	E	D / M	E	C	E / C
Packaging	BGA / LGA	TO-247/220 PQFN88	GaNpx™	VQFM / QFM	DFN-8	All-switch	-	TO-220	-
Thermal Management	Heatsink or PCB	Heatsink or PCB	Heatsink or PCB	Heatsink or PCB	Heatsink or PCB	Heatsink or PCB	-	-	-
Availability	Yes	Yes	Yes	Yes	Yes	Yes	No	No	No
Comment	Low voltage No packaging	Conventional packaging	-	Integrated gate driver	Limited options	High gate threshold voltage SiC diode packaged	1.5 kV Vertical GaN	GaN PSJ-FET	-

E – normally-off (enhancement mode) / D – normally-on (depletion mode) / C – normally-off (cascode) / M – normally-on (MISHEMT)

V. ELECTRIC MOTORS FOR ELECTRO-HYDROSTATIC ACTUATORS WITH IMDS

Four different types of electric machine topologies are potentially good candidates for EHA applications, which are induction machine (IM) [57]–[60], surface and interior PM machine [6], [10], [61]–[63], and switched reluctance machine (SRM) [64]–[67].

A. Performance Evaluation for EHA

For EHA applications, fast torque response with good cyclic performance is the highest priority among other requirements. The fast torque response helps to improve the stiffness of the EHA system, and the cyclic performance is a critical attribute for fail-safe operation. In this section, torque response and cyclic performance of four different electric machines are thoroughly reviewed and compared.

Field-oriented control [68], [69] and direct torque control [70] are widely used for IMs. The deadbeat direct torque and flux control (DB-DTFC), which is well-known for the fastest torque response, has been gaining popularity in a number of applications [71]–[73]. DB-DTFC has also been applied to PM machines, which provides significantly improved torque response [74], [75]. The SRMs typically do not have as fast torque response as the other three machine topologies due to the unique drive topology and the operating principle. In [63], a novel direct instantaneous control of SRM for the hydraulic pump system was proposed. Even though the authors claimed an improvement in the SRM response, its response time is still in the range of 100 ms.

As for the cyclic performance, the IMs have been used in many applications with repetitive motions, such as EH actuators, washing machines, and manufacturing lines. In spite of the technical maturity and robustness of IMs, the system efficiency of EHA with IMs is significantly lower (10%–20%) than that of the EHA with PM machines [76]. The PM machines are being dominantly used in EHA applications due to its high efficiency, high torque density, and fast torque response. Nevertheless, it requires special attention to prevent the rotor overheating, which causes an irreversible demagnetization. The SRMs have robust rotor structures and the inherent fault tolerance capability, which are attractive for EHA applications. However, the highly nonlinear characteristics and high torque ripple are the main drawbacks of SRMs. Much effort has been made in recent years to improve the performance of SRMs [77], torque ripple [78], and acoustic noise [79], which make them more appealing to EHA applications.

B. Challenges and Opportunities for IMDs

Four different types of motors (IM [3], [4], [24], [32], [34], surface permanent magnet motor [3], [5], [26]–[30], [33], IPM [35], and SRM [23], [25], [31]) have been reported in the literature for IMD application. The IMs typically have the relatively long winding overhang, which gives extra space for power electronics for ASM, as shown in Fig. 6(c). In this case, a sophisticated thermal shielding between the stator winding and power electronics is required [3]. A number of thermal analysis and cooling methods have been investigated for IMD application in [3], [23], [35], and [80]–[82], where integrated cooling systems for both electric motors and drive are investigated. The modularity of IMs is lower than that of other types of motors unless multiple three-phase inverter modules are used as introduced in [4].

The PM machines with fractional-slot concentrated winding (FSCW) are becoming increasingly more popular due to their high slot fill factor, short-end turns, high efficiency, and power density [83]. The FSCW also provides high modularity, which makes it more suitable for IMMD application [5]. The challenges associated with IMMDs with the PM machines are the implementation of a distributed control and communication systems with multiple controllers [84]. Each inverter modules need to be synchronized, and the master controller should read the measured current, estimate the output commands, and send them to each module within a time step of a pulsewidth modulation. In [85], multiple DSPs and field-programmable gate arrays with a master/slave architecture and fiber-optic links have been proposed and implemented for cascaded multilevel converters, which is applicable in IMMD application as shown in [35]. The other challenge associated with the IMMDs with the PM machines is the disconnection of inverter modules when a fault occurs. Since rotor magnetic flux cannot be turned OFF, the faulty inverter modules need to be safely disconnected from the remaining healthy modules to prevent uncontrolled generator operation. Series winding TRIACs [52], [86], ac, and dc circuit breaker

are the viable options with the increased system complexity, cost, and volume. The other simple solution is to implement a fuse in series with dc-link capacitor as reported in [87].

The SRMs have the highest modularity among other machine types due to the magnetic and electric independency of each phase winding. It is not required to disconnect any faulty module due to the absence of the rotor magnet. The challenges of IMDs with SRMs are the design of the high-power density inverter modules for the compact integration and high mechanical stress on the power electronics from the motor vibration.

VI. Conclusion

This paper investigates the high-performance EHA system with the IMDs and WBG device technologies. The state-of-the-art actuation systems, IMDs, WBG devices, and electric machines are reviewed and summarized in detail.

The IMDs offer numerous benefits including high power density and fault-tolerant operation, which are becoming more important in the individualized EHA systems. The conceptual illustrations of four different IMD configurations are presented including their example designs. The efficiency and device characteristics of the WBG-based IMDs are also reviewed in comparison with the conventional Si technology, in which the WBG devices outperform especially in a high switching frequency and light-load operation.

The growing demands of high power density and high-temperature operation in the EHA can certainly be satisfied with the emerging power electronics and motor design technologies suggested in this paper.

References

[1] D. Throne, F. Martinez, R. Marguire, and D. Arens, "Integrated motor/drive technology with Rockwell connectivity," Rexroth, Bosch Group, Lohr am Main, Germany, Tech. Rep. [Online]. Available: http://www.cmafh.com/enewsletter/PDFs/IntegratedMotorDrives.pdf

[2] M. März, E. Schimanek, and M. Billmann, "Towards an integrated drive for hybrid traction," in *Proc. CPES Power Electron. Conf.*, 2005, pp. 1–5.

[3] M. März, M. H. Poech, E. Schimanek, and A. Schletz, "Mechatronic integration into the hybrid powertrain—The thermal challenge," in *Proc. Int. Conf. Automot. Power Electron.*, 2006, pp. 1–6.

[4] J. Wang, Y. Li, and Y. Han, "Integrated modular motor drive design with GaN power FETs," *IEEE Trans. Ind. Appl.*, vol. 51, no. 4, pp. 3198–3207, Jul./Aug. 2015.

[5] A. Shea and T. M. Jahns, "Hardware integration for an integrated modular motor drive including distributed control," in *Proc. Energy Convers. Congr. Expo. (ECCE)*, Sep. 2014, pp. 4881–4887.

[6] H. Zhang and J. Wang, "Active steering actuator fault detection for an automatically-steered electric ground vehicle," *IEEE Trans. Veh. Technol.*, vol. 66, no. 5, pp. 3685–3702, May 2017.

[7] F. Meng, H. Zhang, D. Cao, and H. Chen, "System modeling and pressure control of a clutch actuator for heavy-duty automatic transmission systems," *IEEE Trans. Veh. Technol.*, vol. 65, no. 7, pp. 4865–4874, Jul. 2016.

[8] W. Sun, H. Pan, and H. Gao, "Filter-based adaptive vibration control for active vehicle suspensions with electrohydraulic actuators," *IEEE Trans. Veh. Technol.*, vol. 65, no. 6, pp. 4619–4626, May 2016.

[9] I. Martins, J. Esteves, G. D. Marques, and F. Pina da Silva, "Permanent-magnets linear actuators applicability in automobile active suspensions," *IEEE Trans. Veh. Technol.*, vol. 55, no. 1, pp. 86–94, Jan. 2006.

[10] T. A. Minav, C. Bonato, P. Sainio, and M. Pietola, "Efficiency of direct driven hydraulic drive for non-road mobile working machines," in *Proc. Int. Conf. Elect. Mach.*, Sep. 2014, pp. 2431–2435.

[11] D. Woodburn *et al.*, "High-performance electromechanical actuator dynamic heat generation modeling," *IEEE Trans. Aerosp. Electron. Syst.*, vol. 50, no. 1, pp. 530–541, Jan. 2014.

[12] S. C. Jensen, G. D. Jenney, and D. Dawson, "Flight test experience with an electromechanical actuator on the F-18 systems research aircraft," in *Proc. Digit. Avionics Syst. Conf.*, Oct. 2000, pp. 2E3-1–2E3-10.

[13] J.-C. Derrien and S. D. Sécurité, "Electromechanical actuator (EMA) advanced technologies for flight controls," in *Proc. Int. Congr. Aeronaut. Sci.*, 2012, pp. 1–10.

[14] T. A. Minav, J. J. Pyrhonen, and L. I. E. Laurila, "Permanent magnet synchronous machine sizing: Effect on the energy efficiency of an electro-hydraulic forklift," *IEEE Trans. Ind. Electron.*, vol. 59, no. 6, pp. 2466–2474, Jun. 2011.

[15] S. Habibi and A. Goldenberg, "Design of a new high-performance electrohydraulic actuator," *IEEE/ASME Trans. Mechatronics*, vol. 5, no. 2, pp. 158–164, Jun. 2000.

[16] D. van den Bossche, "The A380 flight control electrohydrostatic actuators, achievements and lessons learnt," in *Proc. Int. Congr. Aeronaut. Sci.*, 2006, pp. 1–8.

[17] S. Vladimirov and S. Forde, "Demonstration program to design, manufacture and test an autonomous electro-hydrostatic actuator to gimbal large booster-class engines," in *Proc. AIAA/ASME/SAE/ASEE Joint Propulsion Conf. Exhibit*, 2006, p. 1–6.

[18] J. Weber *et al.*, "Novel system architectures by individual drives," in *Proc. Int. Fluid Power Conf.*, 2016, pp. 29–62.

[19] J. Lodewyks and P. Zurbrügg, "Decentralized energy-saving hydraulic concepts for mobile working machines," in *Proc. IFK*, 2016, pp. 79–90.

[20] K. Rongjie, J. Zongxia, W. Shaoping, and C. Lisha, "Design and simulation of electro-hydrostatic actuator with a built-in power regulator," *Chin. J. Aeronaut.*, vol. 22, no. 6, pp. 700–706, Dec. 2009.

[21] R. Abebe *et al.*, "Integrated motor drives: State of the art and future trends," *IET Electr. Power Appl.*, vol. 10, no. 8, pp. 757–771, Sep. 2016.

[22] N. R. Brown, T. M. Jahns, and R. D. Lorenz, "Power converter design for an integrated modular motor drive," in *Proc. Ind. Appl. Annu. Meeting*, Sep. 2007, pp. 1322–1328.

[23] A. Tenconi, F. Profumo, S. E. Bauer, and M. D. Hennen, "Temperatures evaluation in an integrated motor drive for traction applications," *IEEE Trans. Ind. Electron.*, vol. 55, no. 10, pp. 3619–3626, Oct. 2008.

[24] *Drive Components for Hybrid and Electric Vehicles—SIVETEC*. [Online]. Available: http://w3.siemens.com/topics/global/en/electromobility/pages/powertrain-ecar.aspx

[25] *SR Motor Systems With Integrated SiC-Based Inverters*. [Online]. Available: http://www.nidec.com/en-NA/technology/rd/sic/

[26] J. J. Wolmarans, M. B. Gerber, H. Polinder, S. W. H. de Haan, J. A. Ferreira, and D. Clarenbach, "A 50 kW integrated fault tolerant permanent magnet machine and motor drive," in *Proc. IEEE Power Electron. Specialists Conf.*, Jun. 2008, pp. 345–351.

[27] H. Hijikata and K. Akatsu, "Design and online winding reconfigurations method of MATRIX motor," in *Proc. IEEE 7th Int. Power Electron. Motion Control Conf.*, Sep. 2012, pp. 713–718.

[28] B. J. Sykora, "Development of demonstrator model of an integrated modular motor drive," M.S. thesis, ECE, UW-Madison, Madison, WI, USA, 2008.

[29] A. L. Fuerback, T. B. Soeiro, M. J. Jacoboski, M. L. Heldwein, and A. J. Perin, "Integrated motor drive design for an all-electric boat," in *Proc. PCIM South Amer.*, 2014, pp. 1–8.

[30] *Yaskawa to Launch the World's First GaN Power Semiconductor-Equipped Servo Motor With Built-in Amplifier*. [Online]. Available: https://www.yaskawa.co.jp/en/newsrelease/product/18047

[31] M. D. Hennen, M. Niessen, C. Heyers, H. J. Brauer, and R. W. De Doncker, "Development and control of an integrated and distributed inverter for a fault tolerant five-phase switched reluctance traction drive," *IEEE Trans. Power Electron.*, vol. 27, no. 2, pp. 547–554, Feb. 2012.

[32] G. Su, L. Tang, C. Ayers, and R. Wiles, "An inverter packaging scheme for an integrated segmented traction drive system," in *Proc. Energy Convers. Congr. Expo. (ECCE)*, Sep. 2013, pp. 2799–2804.

[33] F. Hilpert, K. Brinkfeldt, and S. Arenz, "Modular integration of a 1200 v SiC inverter in a commercial vehicle wheel-hub drivetrain," in *Proc. Electr. Drives Prod. Conf. (EDPC)*, Sep./Oct. 2014, pp. 1–8.

[34] P. W. Wheeler *et al.*, "A fully integrated 30 kW motor drive using matrix converter technology," in *Proc. Eur. Conf. Power Electron. Appl.*, Sep. 2005, pp. 1–9.

[35] B. Ahmadi, J. Espina, L. de Lillo, R. Abebe, L. Empringham, and C. M. Johnson, "Next generation integrated drive: A novel thermal and electrical integration technique for high power density converters used in automotive drive systems," in *Proc. 9th Int. Conf. Power Electron., Mach. Drives (PEMD)*, 2018, pp. 1–5.

[36] A. Q. Huang, "Power semiconductor devices for smart grid and renewable energy systems," *Proc. IEEE*, vol. 105, no. 11, pp. 2019–2047, Nov. 2017.

[37] P. Czyz, A. Reinke, A. Cichowski, and W. Sleszynski, "Performance comparison of a 650 V GaN SSFET and CoolMOS," in *Proc. IEEE 10th Int. Conf. Compat., Power Electron. Power Eng.*, Jun./Jul. 2016, pp. 438–443.

[38] T. Bertelshofer, R. Horff, A. März, and M.-M. Bakran, "A performance comparison of a 650 V Si IGBT and SiC MOSFET inverter under automotive conditions," in *Proc. PCIM Eur.*, May 2016, pp. 1–6.

[39] T. Heckel, C. Rettner, and M. März, "Fundamental efficiency limits in power electronic systems," in *Proc. IEEE Int. Telecommun. Energy Conf.*, Oct. 2015, pp. 1–6.

[40] W. Lee, S. Li, D. Han, B. Sarlioglu, T. A. Minav, and M. Pietola, "Achieving high-performance electrified actuation system with integrated motor drive and wide bandgap power electronics," in *Proc. Eur. Conf. Power Electron. Appl. (EPE ECCE Eur.)*, Sep. 2017, pp. 1–10.

[41] D. Han, A. Ogale, Y. Li, and B. Sarlioglu, "Efficiency characterization and thermal study of GaN based 1 kW inverter," in *Proc. Appl. Power Electron. Conf. Expo. (APEC)*, Mar. 2014, pp. 2344–2350.

[42] D. Han, J. Noppakunkajorn, and B. Sarlioglu, "Comprehensive efficiency, weight, and volume comparison of SiC- and Si-based bidirectional DC–DC converters for hybrid electric vehicles," *IEEE Trans. Veh. Technol.*, vol. 63, no. 7, pp. 3001–3010, Sep. 2014.

[43] M. M. Swamy, J. Kang, and K. Shirabe, "Power loss, system efficiency, and leakage current comparison between Si IGBT VFD and SiC FET VFD with various filtering options," *IEEE Trans. Ind. Appl.*, vol. 51, no. 5, pp. 3858–3866, Sep./Oct. 2015.

[44] K. Shirabe *et al.*, "Efficiency comparison between Si-IGBT-based drive and GaN-based drive," *IEEE Trans. Ind. Appl.*, vol. 50, no. 1, pp. 566–572, Jan./Feb. 2014.

[45] K. Shirabe *et al.*, "Design of 400V class inverter drive using SiC 6-in-1 power module," in *Proc. Energy Convers. Congr. Expo. (ECCE)*, Sep. 2013, pp. 2363–2370.

[46] K. Shirabe *et al.*, "Advantages of high frequency PWM in AC motor drive applications," in *Proc. Energy Convers. Congr. Expo. (ECCE)*, Sep. 2012, pp. 2977–2984.

[47] A. G. Sarigiannidis, M. E. Beniakar, P. E. Kakosimos, A. G. Kladas, L. Papini, and C. Gerada, "Fault tolerant design of fractional slot winding permanent magnet aerospace actuator," *IEEE Trans. Transport. Electrific.*, vol. 2, no. 3, pp. 380–390, Sep. 2016.

[48] B. Vaseghi, N. Takorabet, J. P. Caron, B. Nahid-Mobarakeh, F. Meibody-Tabar, and G. Humbert, "Study of different architectures of fault-tolerant actuator using a two-channel PM motor," *IEEE Trans. Ind. Appl.*, vol. 47, no. 1, pp. 47–54, Jan./Feb. 2011.

[49] F. Richardeau, J. Mavier, H. Piquet, and G. Gateau, "Fault-tolerant inverter for on-board aircraft EHA," in *Proc. Eur. Conf. Power Electron. Appl.*, Sep. 2007, pp. 1–9.

[50] C. Gerada, K. Bradley, X. Huang, A. Goodman, C. Whitley, and G. Towers, "A 5-phase fault-tolerant brushless permanent magnet motor drive for an aircraft thin wing surface actuator," in *Proc. IEEE Int. Electr. Mach. Drives Conf.*, May 2007, pp. 1643–1648.

[51] B. A. Welchko, T. M. Jahns, and T. A. Lipo, "Short-circuit fault mitigation method for interior PM synchronous machine drives using six-leg inverters," in *Proc. IEEE 35th Annu. Power Electron. Spec. Conf.*, Jun. 2004, pp. 2133–2139.

[52] B. A. Welchko, T. A. Lipo, T. M. Jahns, and S. E. Schulz, "Fault tolerant three-phase AC motor drive topologies: A comparison of features, cost, and limitations," *IEEE Trans. Power Electron.*, vol. 19, no. 4, pp. 1108–1116, Jul. 2004.

[53] F. Meinguet and J. Gyselinck, "Control strategies and reconfiguration of four-leg inverter PMSM drives in case of single-phase open-circuit faults," in *Proc. IEEE Int. Electr. Mach. Drives Conf.*, May 2009, pp. 299–304.

[54] R. L. A. Ribeiro, C. B. Jacobina, A. M. N. Lima, and E. R. C. da Silva, "A strategy for improving reliability of motor drive systems using a four-leg three-phase converter," in *Proc. IEEE APEC*, Mar. 2001, pp. 385–391.

[55] F. Meinguet, P. Sandulescu, X. Kestelyn, and E. Semail, "A method for fault detection and isolation based on the processing of multiple diagnostic indices: Application to inverter faults in AC drives," *IEEE Trans. Veh. Technol.*, vol. 62, no. 3, pp. 995–1009, Mar. 2013.

[56] B. Wrzecionko, J. Biela, and J. W. Kolar, "SiC power semiconductors in HEVs: Influence of junction temperature on power density, chip utilization and efficiency," in *Proc. Annu. Conf. IEEE Ind. Electron.*, Nov. 2009, pp. 3834–3841.

[57] A. Vakilian-Zand, S. Mohammadi, J. S. Moghani, and M. Mirsalim, "Sensitivity analysis and performance optimization of an industrial squirrel-cage induction motor used for a 150 HP floating pump," in *Proc. 5th Annu. Int. Power Electron., Drive Syst. Technol. Conf. (PEDSTC)*, Feb. 2014, pp. 579–584.

[58] M. S. Miranda, R. O. C. Lyra, and S. R. Silva, "An alternative isolated wind electric pumping system using induction machines," *IEEE Trans. Energy Convers.*, vol. 14, no. 4, pp. 1611–1616, Dec. 1999.

[59] P. Gogolyuk, V. Lysiak, and I. Grinberg, "Influence of frequency control strategies on induction motor-centrifugal pump unit and its modes," in *Proc. IEEE Int. Symp. Ind. Electron.*, Jun./Jul. 2008, pp. 656–661.

[60] T. A. Minav, J. J. Pyrhönen, and L. I. E. Laurila, "Induction machine drive in energy efficient industrial forklift," in *Proc. 21st Int. Symp. Power Electron. Power Electron., Elect. Drives, Autom. Motion (SPEEDAM)*, Jun. 2012, pp. 415–419.

[61] A. Al-Timimy *et al.*, "Design and optimization of a high power density machine for flooded industrial pump," in *Proc. 22nd Int. Conf. Elect. Mach. (ICEM)*, Sep. 2016, pp. 1480–1486.

[62] A. N. A. Hermann, N. Mijatovic, and M. L. Henriksen, "Topology optimisation of PMSM rotor for pump application," in *Proc. 22nd Int. Conf. Elect. Mach. (ICEM)*, Sep. 2016, pp. 2119–2125.

[63] T. Minav, L. Laurila, and J. Pyrhönen, "Energy recovery efficiency comparison in an electro-hydraulic forklift and in a diesel hybrid heavy forwarder," in *Proc. SPEEDAM*, Jun. 2010, pp. 574–579.

[64] H. Yamai, M. Kaneda, K. Ohyama, Y. Takeda, and N. Matsui, "Optimal switched reluctance motor drive for hydraulic pump unit," in *Proc. Conf. Rec. IEEE Ind. Appl. Conf. 35th IAS Annu. Meeting World Conf. Ind. Appl. Elect. Energy*, Oct. 2000, pp. 1555–1562.

[65] S.-H. Lee, Y.-J. An, D.-H. Lee, and J.-W. Ahn, "Performance of SR drive for hydraulic pump," *J. Electr. Eng. Technol.*, vol. 2, no. 1, pp. 55–60, 2007.

[66] B. J. Szymanski, K. Kompa, N. Michalke, H. Kuss, and U. Schuffenhauer, "Power electronic converter for the reluctance pump drive," in *Proc. 13th Int. Power Electron. Motion Control Conf.*, Sep. 2008, pp. 695–698.

[67] J. Liang, D.-H. Lee, J.-W. Ahn, and Y.-J. An, "A novel direct instantaneous pressure control of hydraulic pump system with SRM drive," in *Proc. 7th Int. Conf. Power Electron. (ICPE)*, Oct. 2008, pp. 650–654.

[68] R. Bojoi, P. Guglielmi, and G.-M. Pellegrino, "Sensorless direct field-oriented control of three-phase induction motor drives for low-cost applications," *IEEE Trans. Ind. Appl.*, vol. 44, no. 2, pp. 475–481, Mar./Apr. 2008.

[69] D. M. de la Peña, T. Alamo, D. R. Ramírez, and E. F. Camacho, "Min-max model predictive control as a quadratic program," *IFAC Proc. Vol.*, vol. 38, no. 1, pp. 263–268, 2005.

[70] K. Matsuse, T. Yoshizumi, S. Katsuta, and S. Taniguchi, "High-response flux control of direct-field-oriented induction motor with high efficiency taking core loss into account," *IEEE Trans. Ind. Appl.*, vol. 35, no. 1, pp. 62–69, Jan. 1999.

[71] B. H. Kenny and R. D. Lorenz, "Stator- and rotor-flux-based deadbeat direct torque control of induction machines," *IEEE Trans. Ind. Appl.*, vol. 39, no. 4, pp. 1093–1101, Jul. 2003.

[72] Y. Wang, T. Ito, and R. D. Lorenz, "Loss manipulation capabilities of deadbeat direct torque and flux control induction machine drives," *IEEE Trans. Ind. Appl.*, vol. 51, no. 6, pp. 4554–4566, Nov./Dec. 2015.

[73] D. Casadei, F. Profumo, G. Serra, and A. Tani, "FOC and DTC: Two viable schemes for induction motors torque control," *IEEE Trans. Power Electron.*, vol. 17, no. 5, pp. 779–787, Sep. 2002.

[74] J. S. Lee, R. D. Lorenz, and M. A. Valenzuela, "Time-optimal and loss-minimizing deadbeat-direct torque and flux control for interior permanent-magnet synchronous machines," *IEEE Trans. Ind. Appl.*, vol. 50, no. 3, pp. 1880–1890, May 2014.

[75] A. D. Alexandrou, N. K. Adamopoulos, and A. G. Kladas, "Development of a constant switching frequency deadbeat predictive control technique for field-oriented synchronous permanent-magnet motor drive," *IEEE Trans. Ind. Electron.*, vol. 63, no. 8, pp. 5167–5175, Aug. 2016.

[76] T. A. Minav, L. I. E. Laurila, and J. J. Pyrhönen, "Effect of driving electric machine type on the system efficiency of an industrial forklift," in *Proc. Int. Conf. Electr. Mach.*, 2012, pp. 1964–1970.

[77] P. C. Desai, M. Krishnamurthy, N. Schofield, and A. Emadi, "Novel switched reluctance machine configuration with higher number of rotor poles than stator poles: Concept to implementation," *IEEE Trans. Ind. Electron.*, vol. 57, no. 2, pp. 649–659, Feb. 2010.

[78] J. Ye, B. Bilgin, and A. Emadi, "An extended-speed low-ripple torque control of switched reluctance motor drives," *IEEE Trans. Power Electron.*, vol. 30, no. 3, pp. 1457–1470, Mar. 2015.

[79] M. Takiguchi, H. Sugimoto, N. Kurihara, and A. Chiba, "Acoustic noise and vibration reduction of SRM by elimination of third harmonic component in sum of radial forces," *IEEE Trans. Energy Convers.*, vol. 30, no. 3, pp. 883–891, Sep. 2015.
[80] R. Abebe, G. Vakil, G. L. Calzo, C. Gerada, and M. Johnson, "FEA based thermal analysis of various topologies for integrated motor drives (IMD)," in *Proc. IECON*, Nov. 2015, pp. 1976–1981.
[81] S. Pickering, P. Wheeler, F. Thovex, and K. Bradley, "Thermal design of an integrated motor drive," in *Proc. IECON*, Nov. 2006, pp. 4794–4799.
[82] F. Farina, D. Rossi, A. Tenconi, F. Profumo, and S. E. Bauer, "Thermal design of integrated motor drives for traction applications," in *Proc. Eur. Conf. Power Electron. Appl.*, Sep. 2005, pp. 1–10.
[83] P. B. Reddy, A. M. El-Refaie, K. K. Huh, J. K. Tangudu, and T. M. Jahns, "Comparison of interior and surface PM machines equipped with fractional-slot concentrated windings for hybrid traction applications," *IEEE Trans. Energy Convers.*, vol. 27, no. 3, pp. 593–602, Sep. 2012.
[84] A. Shea and T. M. Jahns, "Control challenges and mitigation techniques for sensor errors in modular motor drives with weakly-coupled distributed control architectures," in *Proc. IEEE Int. Electr. Mach. Drives Conf. (IEMDC)*, May 2015, pp. 890–896.
[85] T. Atalik *et al.*, "Multi-DSP and -FPGA-based fully digital control system for cascaded multilevel converters used in FACTS applications," *IEEE Trans. Ind. Informat.*, vol. 8, no. 3, pp. 511–527, Aug. 2012.
[86] F. Wu, P. Zheng, and T. M. Jahns, "Six-phase fault-tolerant permanent magnet motor drives with reduced switch counts: Topology comparisons and hardware demonstration," in *Proc. IEEE Transport. Electrific. Conf. Expo. (ITEC)*, Jun. 2015, pp. 1–6.
[87] M. Villani, M. Tursini, G. Fabri, and L. Castellini, "High reliability permanent magnet brushless motor drive for aircraft application," *IEEE Trans. Ind. Electron.*, vol. 59, no. 5, pp. 2073–2081, May 2012.

Woongkul Lee (S'13) received the B.S. degree in electrical engineering from Yonsei University, Seoul, South Korea, in 2013, and the M.S. degree in electrical engineering from the University of Wisconsin–Madison, Madison, WI, USA, in 2016, where he is currently pursuing the Ph.D. degree with the Department of Electrical and Computer Engineering.

Since 2015, he has been a Research Assistant with the Wisconsin Electric Machines and Power Electronics Consortium, University of Wisconsin–Madison. His current research interests include wide-bandgap device-based power electronics, high-speed electric machines, and drives.

Dr. Lee received the Jeongsong Cultural Foundation Scholarship from 2013 to 2015.

Silong Li (S'12–M'17) received the B.S. degree in electrical and electronics engineering from Xi'an Jiaotong University, Xi'an, China, in 2011, and the M.S. and Ph.D. degrees in electrical and electronics engineering from the University of Wisconsin–Madison, Madison, WI, USA, in 2014 and 2017, respectively.

He is currently a Motor Control Engineer with Ford Motor Company, Dearborn, MI, USA. His current research interests include the design and analysis of novel permanent magnet machines, and high-performance permanent magnet machine control and drive.

Di Han (S'14) received the B.S. degree in electrical engineering from the Huazhong University of Science and Technology, Wuhan, China, in 2011, and the Ph.D. degree in electrical engineering from the University of Wisconsin–Madison, Madison, WI, USA, in 2017.

He was a Research Assistant with the Wisconsin Electric Machines and Power Electronics Consortium, University of Wisconsin–Madison. He is currently a Senior Applications Engineer with Monolithic Power Systems, Inc., San Jose, CA, USA. His current research interests include wide-bandgap device-based power converter design and electromagnetic interference in motor drives.

Bulent Sarlioglu (M'94–SM'13) received the B.S. degree in electrical engineering from Istanbul Technical University, Istanbul, Turkey, in 1990, the M.S. degree in electrical engineering from the University of Missouri–Columbia, Columbia, MO, USA, in 1992, and the Ph.D. degree in electrical engineering from the University of Wisconsin–Madison, Madison, WI, USA, in 1999.

From 2000 to 2011, he was a Staff Systems Engineer with the Aerospace Division, Honeywell International Inc., Torrance, CA, USA. Since 2011, he has been an Assistant Professor with the University of Wisconsin–Madison, and also the Associate Director of the Wisconsin Electric Machines and Power Electronics Consortium. He is the inventor or co-inventor of 16 U.S. patents as well as many international patents. His current research interests include electrical machines, drives, and power electronics.

Dr. Sarlioglu received the Outstanding Engineer Award from Honeywell International Inc., in 2011.

Tatiana A. Minav (M'18) received the M.Sc. degree from the Lappeenranta University of Technology (LUT), Lappeenranta, Finland, in 2008, the M.Sc. degree from Saint-Petersburg State Electrotechnical University LETI, St. Petersburg, Russia, in 2008, and the Dr.Sc. degree from LUT, in 2011.

She has ten-year experience working on improving the efficiency of nonroad mobile working machines. She is currently with the Department of Mechanical Engineering, Aalto University, Helsinki, Finland. Her current research interests include zonal hydraulics, sensorless position control with direct electric drive in hydraulic systems, failure and monitoring systems, thermal hydraulics simulation, and energy recovery systems in nonroad mobile working machines.

Matti Pietola received the Doctor of Technology degree from Aalto University, Helsinki, Finland, in 1989.

During his academic career, he was with the Tampere University of Technology, Tampere, Finland, and Lappeenranta University of Technology, Lappeenranta, Finland. He has been a Professor of mechatronics (fluid power) with the Department of Mechanical Engineering, Aalto University, since 1997. He has an extensive global contact network with both the industry and the academia in the area of fluid power. He has authored or co-authored 130 international scientific papers.